Theory and Practice of Science and Technology
2025, VOL. 6, NO. 8, 44-51
DOI: 10.47297/taposatWSP2633-456909.20250608

Research on Dual-Closed-Loop Speed Control of DC Motor Based on Multi-Level Integral Separation and Genetic Algorithm Optimization

Bin Chen

Zhejiang Sci-Tech University, Hangzhou, Zhejiang, 310018, China

ABSTRACT

In the low-speed operation of the DC motor dual closed-loop speed control system, The PI controller of the speed loop is prone to experiencing integral saturation due to the persistent presence of large errors., which leads to increasing overshoot and prolonged adjustment time, seriously restricting the system performance. To address this issue, this paper proposes an improved speed loop controller. This controller adopts a multi-level integral separation strategy, managing the integral action in stages based on the error magnitude; and innovatively utilizes the genetic algorithm (GA), taking the comprehensive control index (overshoot + adjustment time) as the fitness function, to automatically optimize the multi-level separation thresholds offline. Experiments were conducted on the Matlab/Simulink platform for the 583.3 rpm step start-up condition. The results show that compared with the traditional PI control, single-level integral separation PI control, and multi-level integral separation PI control with manually set thresholds, the proposed GA-optimized multi-level integral separation method can effectively suppress integral saturation, significantly reduce overshoot (nearly zero) and shorten the adjustment time (by approximately 18%). This method effectively solves the low-speed integral saturation problem, significantly improves the dynamic performance and robustness of the system, and provides an automated optimization solution for high-performance low-speed control of DC motors.

KEYWORDS

DC motor; Dual closed-loop speed regulation; Integral saturation; Multi-level integral separation; Genetic algorithm; Parameter optimization; Low-speed control

1 Introduction

DC motors possess outstanding speed regulation performance, strong starting capability and precise torque control ability. These characteristics enable them to have wide applications in automated production lines. According to the public data released by Huajing Industry Research Institute, the market size of DC motors in China was approximately 97.4 billion yuan in 2023, with a year-on-year growth rate of 7.98%. Although in the current era, with the rapid development of technologies such as intelligent manufacturing and Industry 4.0, the control methods of DC motors tend to be diversified, the control method based on dual closed-loop control, due to its simple design and calculation, is still widely used in the speed regulation control of DC motors.

During actual operation, the traditional DC motor dual-loop speed control system generally adopts the engineering design method [1] to design its speed regulator (ASR) and current regulator (ACR). Although the engineering design method has the advantages of clear concepts, easy understanding, simple and easy-to-remember calculation formulas, and wide applicability, it also has some disadvantages, such as excessive overshoot and slow adjustment time when the speed setpoint is low due to the occurrence of integral saturation. Specifically, when the motor starts, brakes, or the load suddenly changes, the initial speed deviation is large, causing the integral term of the PI controller to accumulate rapidly to the saturation limit value. This excessive accumulation leads to significant overshoot in the motor speed, increased adjustment time, and system oscillation, which is particularly prominent in wide-range speed control scenarios.

Traditional anti-saturation methods, such as the integral clipping method, often encounter limitations such as decreased dynamic performance, high parameter dependence, and complex implementation. The classic integral separation method [2] has the basic idea that integral control is introduced only when the controlled quantity approaches the set value, in order to reduce static error and improve control accuracy. Although this can suppress saturation within a certain range, the single fixed threshold setting is difficult to adapt to all operating conditions to achieve optimal control. The subsequent developed multi-level integral separation strategy can provide more precise control, but the selection of thresholds usually relies on experience or extensive trial and error, increasing the design complexity. To address these issues, this paper proposes to introduce the multi-level integral separation strategy into the dual-loop speed regulation system. The integral effect is weakened or removed in stages based on the size of the error, more accurately suppressing saturation. At the same time, to address the difficulty of multi-level threshold optimization, a genetic algorithm is proposed for automated global optimization to obtain the optimal combination of multi-level separation thresholds, systematically solving the problem of low-speed integral saturation and improving control performance.

*** Corresponding Author:** Bin Chen, 1156779576@qq.com

In recent years, many scholars both at home and abroad have proposed methods for integrating intelligent optimization algorithms with traditional control. Yang Shaoyuan et al [3]. proposed a motor speed control strategy based on self-learning of target speed and fuzzy control algorithm in 2023, and the experimental verification showed that this fuzzy control algorithm had a good control effect in the DC speed control system, and performed excellently in terms of motor smoothness. In 2024, Saidong et al [4]. proposed using the improved genetic algorithm to set the parameters of the PI controller, and after experimental verification, it was found that compared with traditional engineering design methods, this method had better setting effects, with faster response speed, better stability and smaller overshoot, and was more suitable for setting the control parameters of the dual-loop speed control system of DC motors. In 2025, G. Saravanan et al [5]. proposed using the Kookaburra optimization algorithm (KOA) and the Red Panda optimization algorithm (RPOA) to solve the controller gain in the DC motor speed control system. After experimental verification, it was found that compared with traditional meta-heuristic algorithms, KOA had a faster rise time and larger bandwidth, and RPOA had a shorter adjustment time. The integration of intelligent algorithms and traditional control strategies has become the mainstream direction for improving the performance of classic control structures.

Among various intelligent optimization algorithms, the Genetic Algorithm (GA) [6] is based on the group search technology. It represents the solution set as a population and iteratively generates a new population through genetic operations such as selection, crossover, and mutation to guide the population to evolve to a state containing the optimal or approximately optimal solution. GA demonstrates efficient, accurate, and robust advantages in multi-objective optimization problems due to its parallel global search capability based on the population, low requirements for the form of the objective function, strong problem representation and coding flexibility, inherent robustness, and ease of integration with other methods. It is particularly suitable for solving complex optimization problems.

This paper first establishes a system mathematical model, then theoretically analyzes the mechanism of integral saturation problem, subsequently proposes an improved strategy combining multi-level integral separation strategy with genetic algorithm optimization, and finally, through experimental comparisons with various benchmark schemes (traditional PI, single-level integral separation PI, multi-level integral separation PI with manually set threshold), verifies the effectiveness and reliability of the proposed method.

2 System modeling and problem analysis

2.1 Mathematical model of a DC motor

To analyze the stability and dynamic performance of the speed control system, a mathematical model reflecting the dynamic physical laws of the system needs to be established. The research object of this paper is the widely used separately excited DC motor, and its dynamic mathematical model is shown in Figure 1.

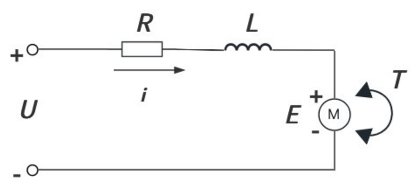

Figure 1 Dynamic mathematical model of separately excited DC motor

Assuming that the armature current is continuous, according to Kirchhoff's Voltage Law, the voltage balance equation of the armature circuit can be obtained:

$$U = Ri + L\frac{di}{dt} + E \tag{1}$$

Under the rated excitation condition, there is:

$$E = C_e n \tag{2}$$

$$T_e = C_m i \tag{3}$$

Ignoring interference factors such as viscous friction and elastic torque, the dynamic equation on the motor shaft is:

$$T_e - T = \frac{GD^2}{375}\frac{dn}{dt} \tag{4}$$

Define the electromagnetic time constant of the armature circuit as T_l and the torque time constant as T_m:

$$T_l = \frac{L}{R} \tag{5}$$

$$T_m = \frac{GD^2 R}{375 C_e C_m} \tag{6}$$

Substituting Equations (2) - (3) and Equations (5) - (6) into Equation (1) and Equation (4), and then simplifying, we obtain:

$$U - E = R(i + T_l \frac{di}{dt}) \tag{7}$$

$$i - i_{dL} = \frac{T_m}{R} \frac{dE}{dt} \tag{8}$$

In the formula:

C_e—— Electromotive force coefficien under rated excitation (N·m/A), related to the structure of the motor and the excitation flux;

T—— Load torque(N·m), including no-load torque;

GD^2—— Flywheel torque ($N{\cdot}m^2$), $GD^2 = 4gJ$;

C_m—— Torque coefficient under rated excitation (N·m/A), $C_m = \frac{30}{\pi} C_e$;

i_{dL}—— Load current (A), $i_{dL} = \frac{T}{C_m}$。

Under zero initial conditions, performing the Laplace transform on Equation (7) yields the transfer function of the armature voltage U(s) - E(s) and the armature current I(s):

$$\frac{I(s)}{U(s) - E(s)} = \frac{1/R}{T_l s + 1} \tag{9}$$

Performing the Laplace transform on Equation (8), we obtain the transfer functions of the armature current I(s) - I_dL(s) and the back electromotive force E(s):

$$\frac{E(s)}{I(s) - I_{dL}(s)} = \frac{R}{T_m s} \tag{10}$$

From Equations (2), (9) and (10), the transfer function model of the DC motor under rated excitation can be obtained, as shown in Figure 2.

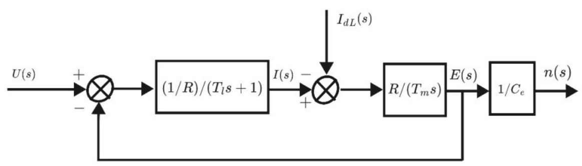

Figure 2 The transfer function model of the DC motor under rated excitation

2.2 Double closed-loop speed control system structure

The double closed-loop speed regulation system consists of two negative feedback loops: the current inner loop and the speed outer loop. The corresponding controllers are respectively called the current regulator (ACR) and the speed loop (ASR), both of which are PI regulators with output limiting (set to [-10, 10] in this paper). The steady-state structure of the system is shown in the system block diagram in Figure 3. In the figure, U_n^* is the speed reference voltage, U_n is the speed feedback voltage, and its deviation ΔU_n serves as the input to ASR; U_i^* is the output of ASR (i. e., the current reference voltage), U_i is the current feedback voltage, and its deviation ΔU_i serves as the input to ACR; K_s is the amplification coefficient of the power electronic converter (UPE); U is the armature voltage; iR is the armature voltage drop; E is the reverse electromotive force; n is the speed; α and β are the speed and current feedback coefficients respectively.

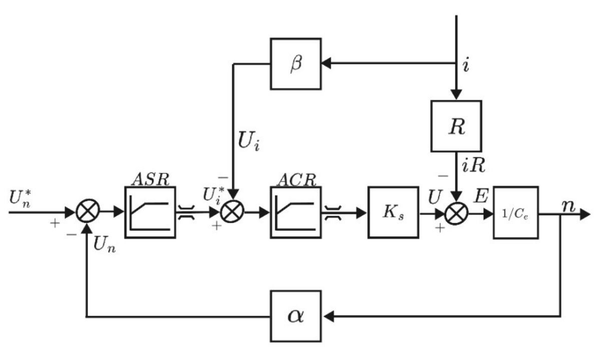

Figure 3 Steady-state structure block diagram of the dual-closed-loop speed control system of the DC motor

Let $W_{ACR}(s)$ and $W_{ASR}(s)$ be the transfer functions of ACR and ASR respectively. The system's dynamic transfer function model can be plotted, as shown in Figure 4.

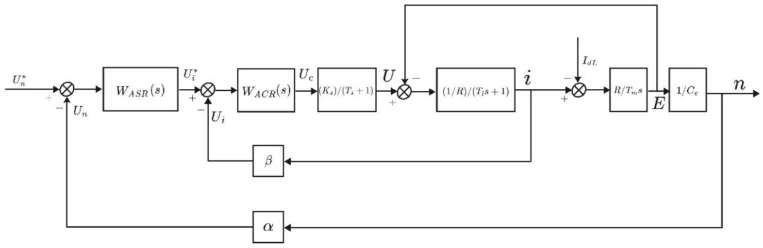

Figure 4 Transfer function model of the dual closed-loop speed control system of the DC motor

2.3 Structure of PI controller

In the double closed-loop speed regulation system, the ASR and ACR usually employ PI controllers. The continuous domain input-output relationship is as follows:

$$U_{out} = K_p U_{in} + \frac{1}{K_i}\int_0^t U_{in}\,dt \tag{11}$$

The transfer function is:

$$W_{PI}(s) = K_p + \frac{1}{K_i s} = \frac{K_p K_i s + 1}{K_i s} \tag{12}$$

In the formula: U_{out} represents the output of the controller; K_p is the proportional gain; K_i is the integral time coefficient (note: some literature defines the integral gain $K_I = \frac{1}{K_i}$, while this article adopts the definitions in Equations (11) and (12)); U_{in} is the input of the controller. The selection of parameters K_p and K_i is of crucial importance. This article follows the engineering design method [1] and approximates the speed loop and current loop as typical I-type systems. Parameter design is carried out using formulas and charts, and the mothod is more convenient compared to classical control theory.

2.4 Analysis of the saturation mechanism of integration

During the motor startup process, the output of ASR rapidly reaches the limit value (saturation state), forcing ACR to maintain the maximum allowable current and driving the rotational speed to rise rapidly. According to the integral control law, as long as the input deviation ΔU_n of ASR is greater than 0, its output U_i^* will continue to increase (limited by the saturation value). Only when $\Delta U_n = 0$, the output stops increasing; when $\Delta U_n < 0$, the output begins to decrease and exits the saturation state. When the actual rotational speed approaches the given rotational speed, ΔU_n decreases, but the integral term of ASR has accumulated a large amount of integral quantity during the saturation period. Therefore, even when $\Delta U_n = 0$, U_i^* still remains at the limit value, causing the current to remain at the maximum and the rotational speed to continue to rise. Only when the actual rotational speed exceeds the given rotational speed (resulting in overshoot), that is, $\Delta U_n < 0$, the integral term begins to accumulate in the reverse direction, and U_i^* is able to exit the saturation state and enter the linear regulation zone, ultimately the rotational speed tends to stabilize.

Since the PI parameters in the ASR are designed based on the rated speed, this results in the fact that when the given speed is relatively low, the ASR integral term will inevitably accumulate to a relatively large value during the saturation period (the integral saturation phenomenon intensifies), leading to a more significant overshoot during low-speed startup. The following text will propose improvement strategies for this issue.

3 Multi-level integral separation and GA optimization strategy design

3.1 The multi-level integral separation principle

The basic idea of integral separation [2] is as follows: when the input deviation of the controller is large, the integral action is disabled to prevent excessive overshoot caused by integral accumulation; when the deviation is small, the integral action is introduced to eliminate the steady-state error and improve the control accuracy.

Single-stage integral separation is achieved by setting a deviation threshold ε: when $|e(k)| \geq \varepsilon$, PD control is adopted to reduce overshoot and achieve a faster response; when $|e(k)| < \varepsilon$, PID control is used to ensure steady-state accuracy.

Multi-level integral separation is achieved by setting multiple thresholds on the basis of a single level, dividing the control interval into multiple sub-intervals, and flexibly choosing different integral strategies according to the actual characteristics of each sub-interval, thereby improving the control effect. This paper adopts a three-level integral separation strategy. The specific steps are as follows:

1) Set two deviation thresholds ε_1 and ε_2;

2) Set the factor γ for weakening the effect of integral:

$$\gamma = \begin{cases} B, & |e(k)| \le \varepsilon_2 \\ A, & \varepsilon_2 < |e(k)| < \varepsilon_1 \\ 0, & \varepsilon_1 \le |e(k)| \end{cases} \tag{13}$$

Equation (13) indicates that when $|e(k)| > \varepsilon_1$ (large deviation), the integral effect is completely removed ($\gamma = 0$) to avoid rapid saturation; when $\varepsilon_2 < |e(k)| < \varepsilon_1$ (medium deviation), a weak integral effect ($\gamma = A < B$) is adopted to accelerate adjustment while suppressing excessive accumulation; when $|e(k)| \le \varepsilon_2$(small deviation), a strong integral effect ($\gamma = B$) is used to ensure steady-state accuracy. The multi-level structure is more flexible and adaptable than the single-level structure.

However, the traditional threshold for integral separation (ε or ε_1,ε_2) is usually set based on manual experience, which is difficult to ensure optimality and requires repeated trial and error. This makes the engineering application cumbersome (especially for complex systems). Therefore, this paper introduces the genetic algorithm (GA) to automatically optimize the combination of optimal thresholds (ε_1, ε_2), thereby saving time and improving the control effect.

3.2 Design and implementation of Genetic Algorithm (GA)

Genetic algorithms[6] are inspired by the theory of biological evolution and are a type of random search algorithm that simulates the mechanisms of natural selection and genetics. The solution process can be summarized as:

1) Initialization: Based on the problem specification, set the population size N, and randomly generate N initial solutions (individuals) to form the initial population. Individuals are usually encoded in binary or real numbers.

2) Fitness evaluation: Define the fitness function Fitness(X) to quantify the degree of adaptation of individual X to the problem environment (the quality of the solution). In minimization problems, the lower the fitness value, the better the individual is.

3) Genetic operation: Selection: Based on the fitness value, select excellent individuals with a certain probability to enter the mating pool; Crossover: For the individuals in the mating pool, perform genetic exchange with a certain probability P_c to generate new individuals. Mutation: Randomly change some of the gene values of the new individuals with a certain probability P_m to increase the diversity of the population.

4) Iterative evolution: New individuals form a new generation of population. Steps 2-3 are repeated until the stopping conditions are met (such as reaching the maximum number of iterations or achieving convergence in fitness).

GA achieves global optimization through group search and genetic operations. Its diversity mechanism can effectively cover the solution space and prevent the problem of artificial trial-and-error from falling into local optimum (see Figure 5 for the process diagram).

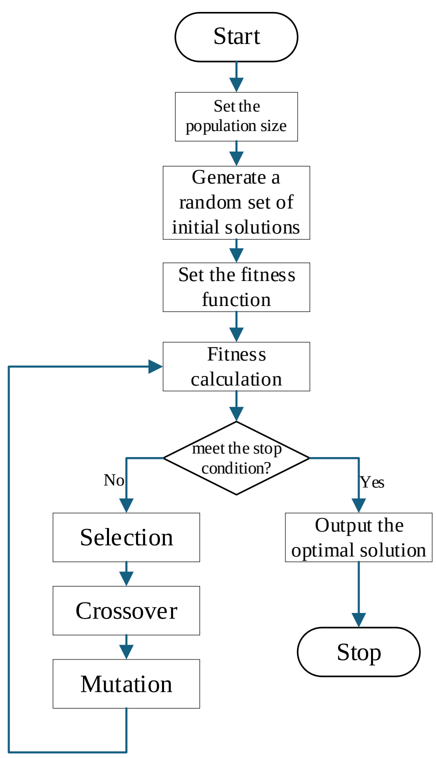

Figure 5 Flowchart of genetic algorithm process

This paper implements the GA design within the MATLAB Optimization Toolbox:

1) Define variables: Create two one-dimensional continuous optimization variables $x(\varepsilon_1)$ and $y(\varepsilon_2)$, with the range of values being [0 10]. The initial values are set to 5 and 1 respectively.

2) Defining the problem: Set the optimization objective to minimize the fitness function:

$$Fitness = \omega_1 * \sigma\% + \omega_2 * t_s \tag{14}$$

Here, $\sigma\%$ represents the overshoot percentage (%), t_s denotes the settling time (s), and ω_1 and ω_2 are the weight coefficients (in this paper, $\omega_1 = 0.7$ and $\omega_2 = 0.3$).

3) Constraint condition: Add the constraint $y \le x$ (that is, $\varepsilon_2 \le \varepsilon_1$).

4) Algorithm selection: The genetic algorithm solver is selected for optimization calculations.

4 Experimental platform and result analysis

4.1 Establishment of simulation model

Based on the transfer function model shown in Figure 4, a dual-loop speed control simulation model for the DC motor was established in MATLAB/Simulink (Figure 6).

The model incorporates an integration separation module (structure shown in Figure 7), whose output determines the weakening factor γ of the ASR integration section. The core simulation parameters are presented in Table 1. The system's real-time rotational speed n was outputed to the MATLAB workspace, and GA calculated the overshoot percentage $\sigma\%$ and the regulation time t_s under the current threshold combination [ε_1, ε_2] based on this, and substituted them into the fitness function (14) for evaluation. GA continuously iterated and optimized the threshold combination.

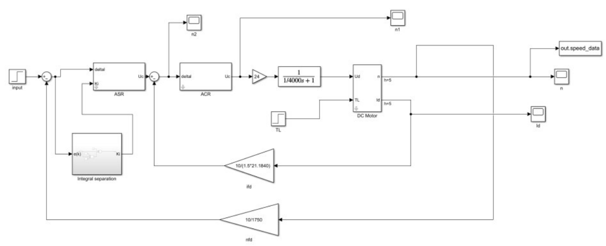

Figure 6 DC motor dual-closed-loop speed regulation simulink simulation model

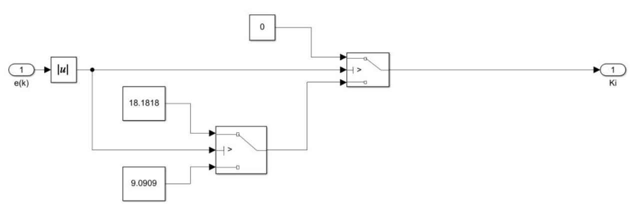

Figure 7 Integral separation module structure

Table 1 Core parameters of the simulation model

Title	Numerical values
Output limit of the regulator	[-10 10]
Rated current of the DC motor	21.184 A
Rated torque of the DC motor	21.4255 (N·m)
Rated rotational speed of the DC motor	1750 r/min
Electromagnetic time constant (T_l)	0.0108 s
Mechanical-electrical time constant (T_m)	0.0569 s
Speed feedback coefficient (α)	0.0057 $(V\cdot\frac{min}{r})$
Current feedback coefficient (β)	0.3147 V/A
Proportional coefficient of the current re-gulator (K_{pi})	0.8240
Integral coefficient of the current regulat-or (K_{ii})	92.5926
Proportional coefficient of the speed regu-lator (K_{pn})	7.0307
The factor (γ) for weakening the effect of integral	B=9.0909,A=18.1818

4.2 Comparison scheme setup

To verify the effectiveness of the proposed method, the following comparison scheme was set up:

Scheme A (Traditional PI): No integral separation module.

Scheme B (Single-stage Integral Separation PI): Manually set a single empirical threshold $\varepsilon = 1.8$.

Scheme C (Manual Multi-level Integral Separation PI): Manually set the threshold combinations $\varepsilon_1 = 1.8$ and $\varepsilon_2 = 1.0$.

Scheme D (GA-optimized multi-level integral separation PI): GA conducts offline optimization of threshold combinations (the optimal results are shown in 4.3).

4.3 Experimental results presentation and analysis

Under no-load conditions, the target speed was 583.33 rpm and the DC motor started from a stationary state. Figure 8 shows the motor speed response curves under the four control schemes. Table 2 compares the dynamic performance indicators (overshoot percentage σ% and regulation time t_s) of each scheme.

Table 2 Dynamic performance comparison of the four schemes (starting at 583.33 rpm)

Scheme	Control strategy	overshoot percentage σ%	regulation time t_s
A	Traditional PI	10.74%	0.340
B	Single-stage Integral Separation PI ($\varepsilon = 1.8$)	6.28%	0.337
C	Manual Multi-level Integral Separa-tion PI ($\varepsilon_1 = 1.8, \varepsilon_2 = 1.0$)	0.63%	0.312
D	GA-optimized multi-level integral separation PI	≈0	0.280

As can be seen from Table 2:

1) The traditional PI control (A) exhibits significant overshoot (10.74%), the longest adjustment time (0.34 seconds), and obvious saturation of the integrator.

2) Single-pole integral separation (B) effectively reduces the overshoot by 6.28% and slightly shortens the regulation time to 0.337 seconds.

3) The multi-level integral separation with manual threshold setting (C) further improves the performance, with the overshoot significantly reduced (by 0.63%) and the regulation time shortened to 0.312 seconds.

4) The GA-optimized multi-stage integration separation scheme (D) proposed in this paper has the best effect, with an almost zero overshoot and a significantly shortened adjustment time to 0.28s (an increase of approximately 18% compared to scheme A). This indicates that the output of the integrator is always within the limiting range, effectively avoiding saturation.

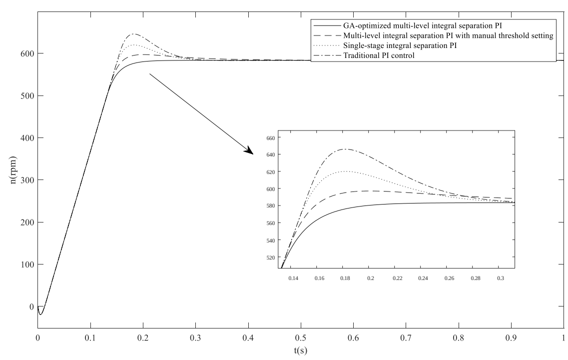

Figure 8 Motor speed variation curve

Figure 9 shows the fitness evolution curve of the GA optimization process. It can be seen that:

In the early stage of evolution, the optimal fitness value dropped sharply from the initial value of 7.48781, indicating that the algorithm conducted efficient global exploration within the search space and quickly approached the optimal region.

The average fitness value decreased rapidly in synchronization, indicating a significant improvement in the overall quality of the population.

After approximately 110 generations, the fitness values began to converge. The optimal fitness eventually stabilized at around 0.0512859 (with fluctuations less than ±0.0005).

The average fitness converged to 0.0513243, with a difference of only 0.0000384 from the optimal fitness, indicating that the population is highly concentrated near the optimal solution.

After 150 generations, the optimal fitness curve almost coincided with the average fitness curve, confirming that the population diversity had been appropriately reduced, and the algorithm had shifted from global exploration to local detailed development.

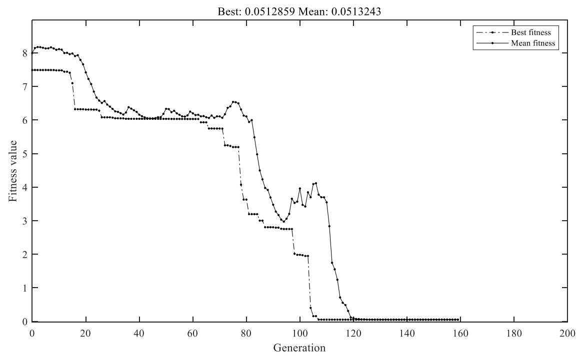

Figure 9 Fitness evolution curve of the GA optimization process

In conclusion, the multi-level integral separation strategy optimized by GA can effectively suppress the low-speed integral saturation problem existing in the DC speed regulation system, significantly improve the dynamic performance (reducing overshoot, shortening adjustment time) and steady-state accuracy, and achieve the automation of the parameter optimization process. However, it should be pointed out that this method also inevitably has limitations, such as the offline optimization time of GA, and its effect depends on the accuracy of the simulation model or experimental platform.

5 Conclusion

This paper addresses the problem of integral saturation in the dual-loop speed control system of DC motors under low-speed conditions, and proposes a solution that combines a multi-level integral separation strategy with genetic algorithm (GA) optimization. The core innovation lies in: using a multi-level structure to finely regulate the intensity of the integral effect; and employing GA to automatically search for the offline optimal combination of separation thresholds (ε_1,ε_2) for integral separation.

Through detailed simulation experiments, the following conclusions were drawn:

1)The proposed method can effectively suppress the integral saturation phenomenon during the low-speed startup process.

2)Compared with traditional PI control, single-machine integral separation PI control, and multi-level integral separation PI control with manual threshold setting, the GA-optimized multi-level integral separation control significantly reduces the overshoot of the low-speed step response (almost zero) and shortens the regulation time (decreasing by approximately 18%).

3)The genetic algorithm provides an efficient and automated global optimization approach for optimizing the thresholds of multi-level integration separation.

This paper provides an effective and highly automated optimization solution for the problem of integral saturation in low-speed control of DC motors. Future research can consider introducing more efficient online optimization algorithms to achieve real-time dynamic adjustment of thresholds, thereby further enhancing the system's adaptability to different operating conditions.

References

[1] Ruan Yi, Yang Ying, Chen Boshi. Automatic Control System for Electric Drive [M]. 5th Edition. Beijing: Mechanical Industry Press, 2020.

[2] Pan Tianhong. Computer Control Technology [M]. 1st Edition. Beijing: Mechanical Industry Press, 2021.

[3] Yang Shaoyuan, Peng Banghuang, Xiong Bin, et al. Research on DC Motor Speed Control Algorithm Based on Fuzzy Control [C]// Chinese Society for Automotive Engineering. 2023 Annual Conference of Chinese Society for Automotive Engineering (Volume 4). BYD Automotive Engineering Research Institute, 2023: 301-310.

[4] Sai Dong, Zhu Kuo, Kong Xiangxuan. Control Parameter Tuning of DC Motor Dual-Closed-loop Speed Regulation System Based on Improved Genetic Algorithm [J]. Automation Application, 2024, 65(04): 29-33 + 36.

[5] Saravanan, G., Pazhanimuthu, C. & Naveen, P. Performance improveme-nt of DC motor control system using PID controller with Kookaburra and Red Panda optimization algorithm. Sci Rep 15, 20021 (2025).

[6] Ren Jia. Intelligent Control Theory and Applications [M]. 1st Edition. Beijing: Mechanical Industry Press, 2024.